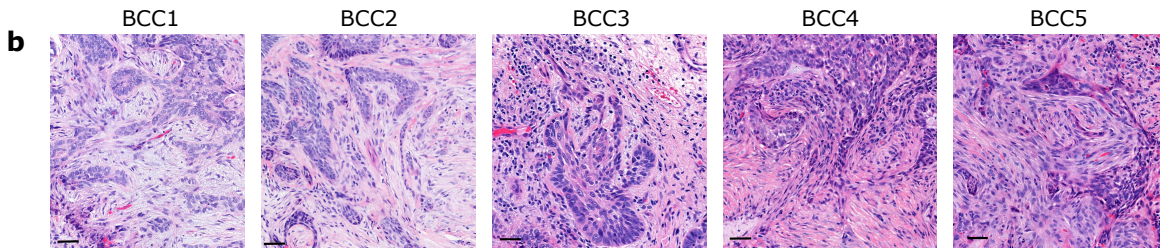


**Integrated multi-omics reveals  
cellular and molecular interactions  
governing the invasive niche of  
basal cell carcinoma**

**SUPPLEMENTARY INFORMATION**

**a**

ID	Diagnosis	Location	Previous treatment	Sample
BCC1	infiltrative BCC	left ear	no	scrRNA-seq
BCC2	infiltrative BCC	forehead	no	scrRNA-seq
BCC3	infiltrative BCC	left cheek	no	scrRNA-seq
BCC4	infiltrative BCC	nose	no	scrRNA-seq
BCC5	infiltrative BCC	nose	no	scrRNA-seq
DSP1	nodular BCC	right leg	no	DSP-seq
DSP2	nodular BCC	scalp	no	DSP-seq
DSP3	nodular BCC	left leg	no	DSP-seq
DSP4	nodular BCC	upper lip	no	DSP-seq
DSP5	nodular BCC	forehead	no	DSP-seq
DSP6	nodular BCC	right cheek	no	DSP-seq
DSP7	infiltrative BCC	left eyebrow	no	DSP-seq
DSP8	infiltrative BCC	right elbow	no	DSP-seq
DSP9	infiltrative BCC	left ear	no	DSP-seq
DSP10	infiltrative BCC	left ear	no	DSP-seq
DSP11	infiltrative BCC	left cheek	no	DSP-seq
DSP12	infiltrative BCC	nose	no	DSP-seq

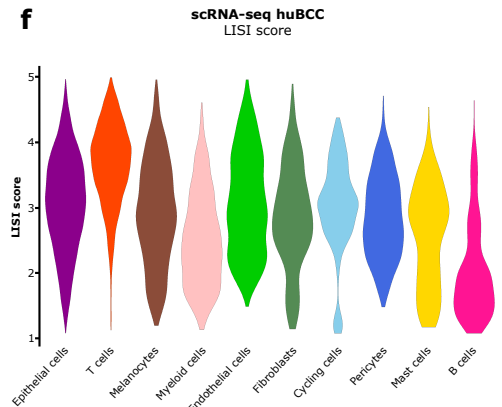
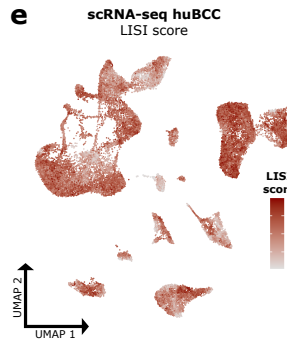
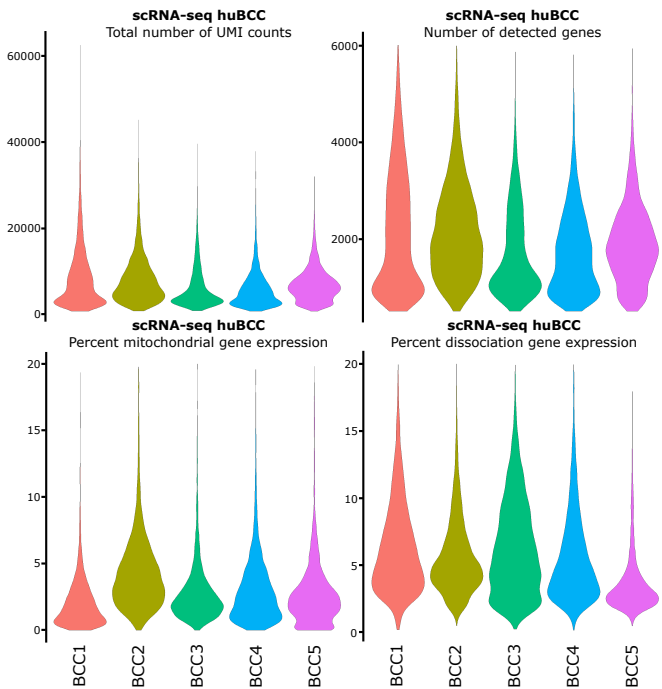


**c**

ID	# cells before filtering	# cells after filtering	# filtered out cells	% filtered out cells
BCC1	5856	5475	381	6.51
BCC2	9109	8562	547	6.01
BCC3	3823	3553	270	7.06
BCC4	6728	6181	547	8.13
BCC5	5267	5039	228	4.33

**d**

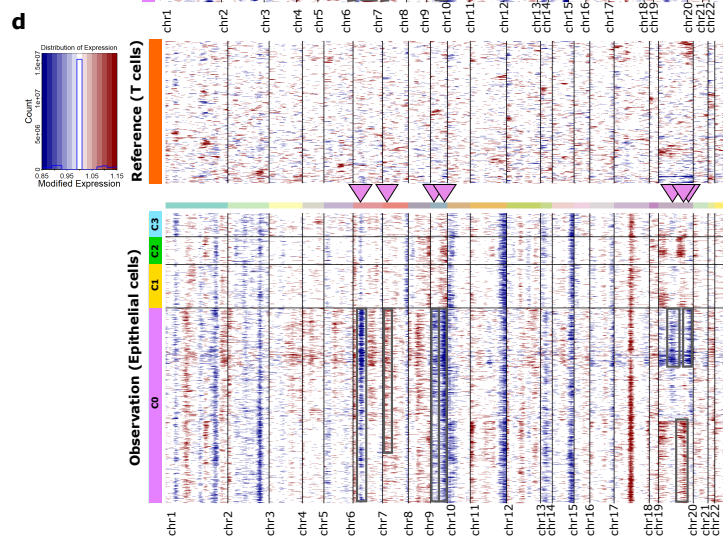
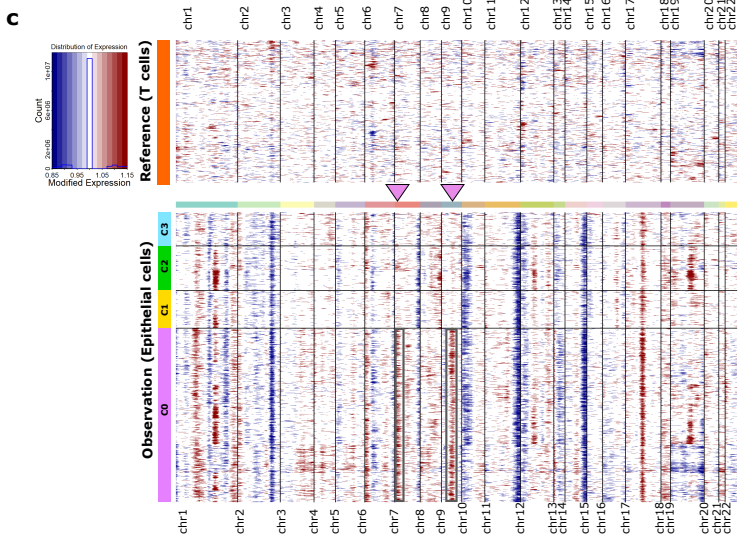
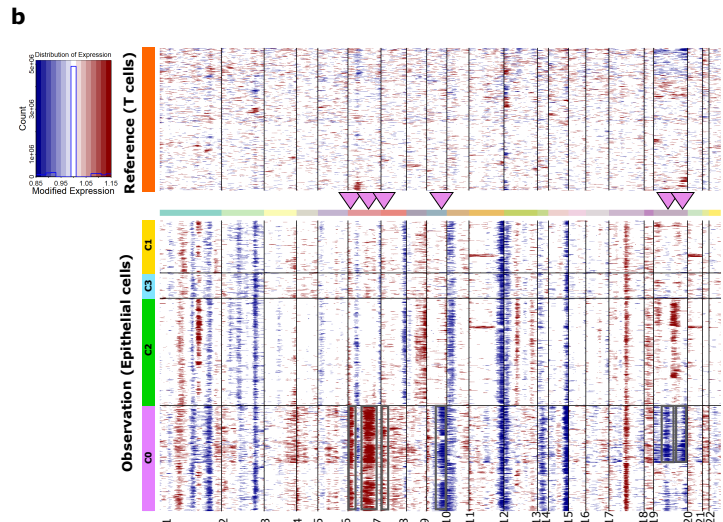
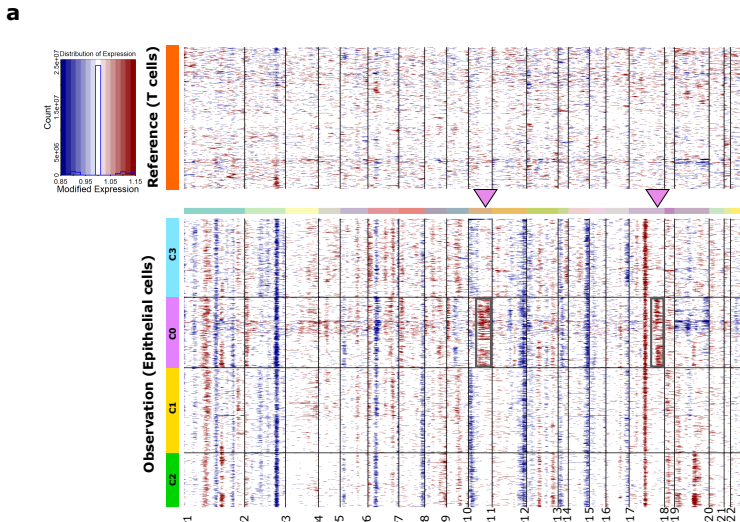
Cell subtype	Number of cells	Percentage
Epithelial cells	14586	50.63
T cells	6565	22.79
Melanocytes	2440	8.47
Myeloid cells	1384	4.80
Endothelial cells	943	3.27
Fibroblasts	809	2.81
Cycling cells	560	1.94
Pericytes	486	1.69
Mast cells	439	1.52
B cells	598	2.08
Total	28810	100.00



**Supplementary Fig. 1 Characteristics of tumor samples and quality controls of scRNA-seq.**

**a)** Table representing the characteristics of the five samples used for scRNA-seq and the twelve samples used for DSP analysis. Patient ages ranged from 49 to 92 years old. **b)** Histology of the five infiltrative human BCCs (huBCCs) selected for scRNA-seq analysis. Scale bars indicate 50  $\mu\text{m}$ . **c)** Table representing the number of cells from each huBCC scRNA-seq sample before and after filtering for low quality cells, the number of filtered out cells and the proportion of filtered out cells relative to the initial number of cells. Violin plots show the total number of UMI counts per cell (upper left), number of detected genes per cell (upper right), percentage of mitochondrial gene expression per cell (lower left) and the percentage of dissociation-associated genes expression per cell (lower right) after integration of the five filtered scRNA-seq huBCC samples. **d)** Table indicating the total number of cells present in individual cell type subpopulations and the proportion of individual subpopulations relative to the total amount of cells in the scRNA-seq dataset. **e)** UMAP plot showing the Local Inverse Simpson's Index (LISI) score of five filtered scRNA-seq huBCC samples after integration. **f)** Violin plots illustrating the LISI score of each cell type subpopulations after integration of the five filtered scRNA-seq huBCC samples.

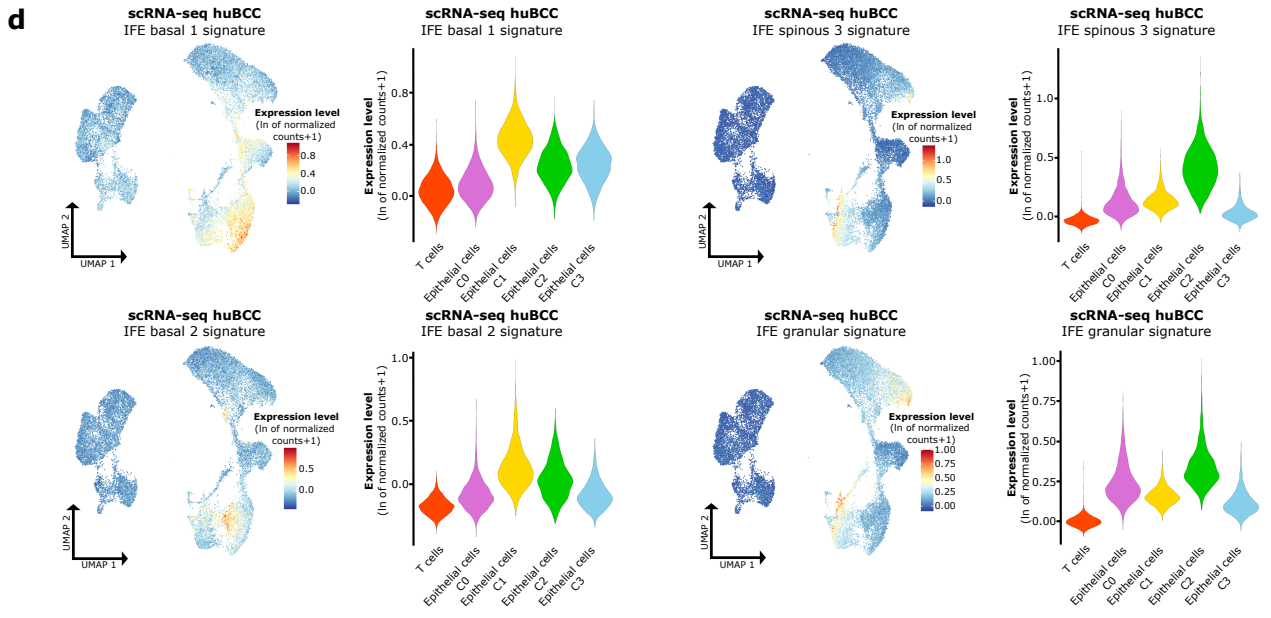
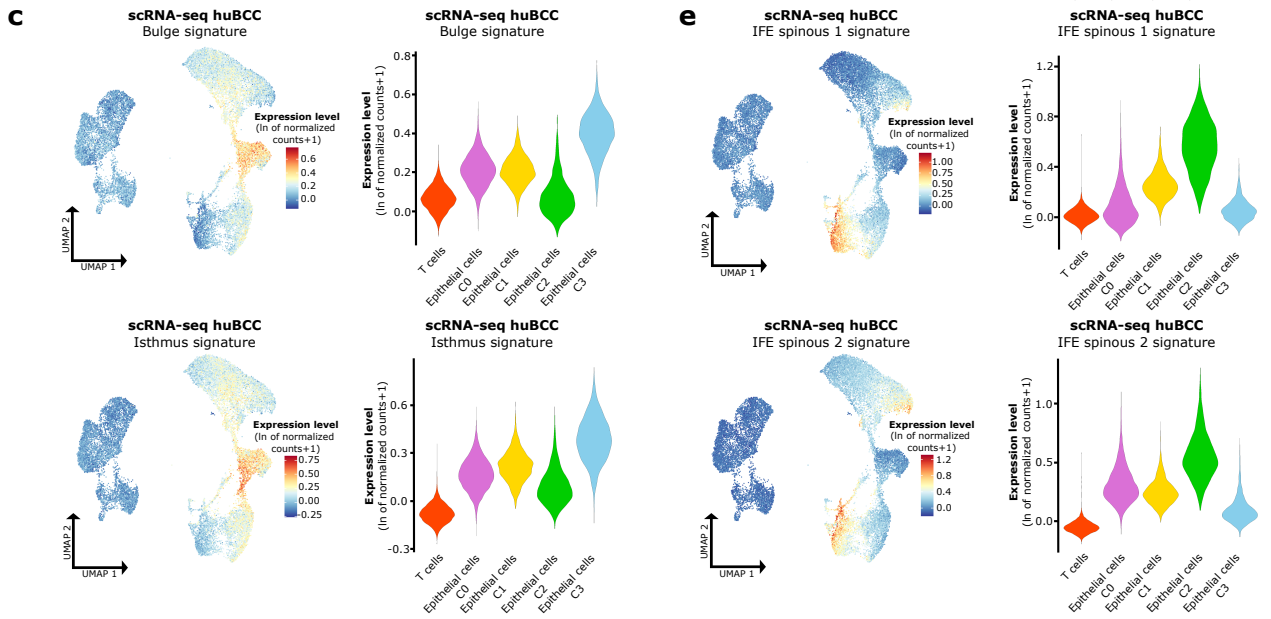
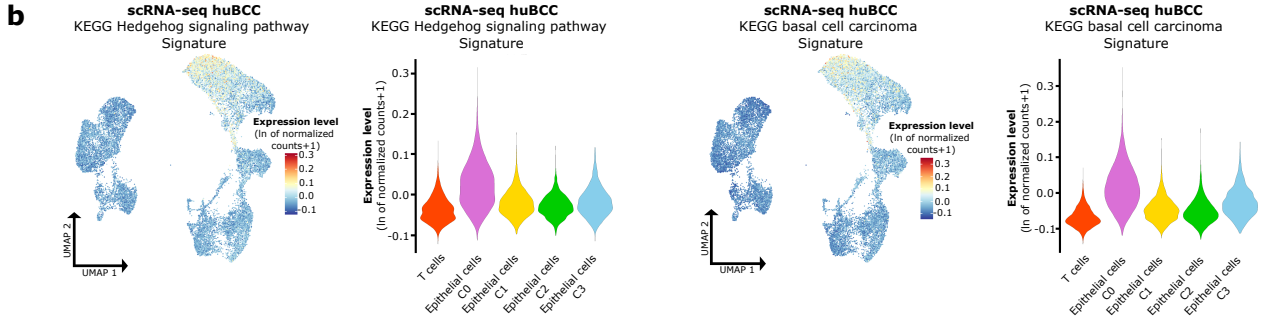
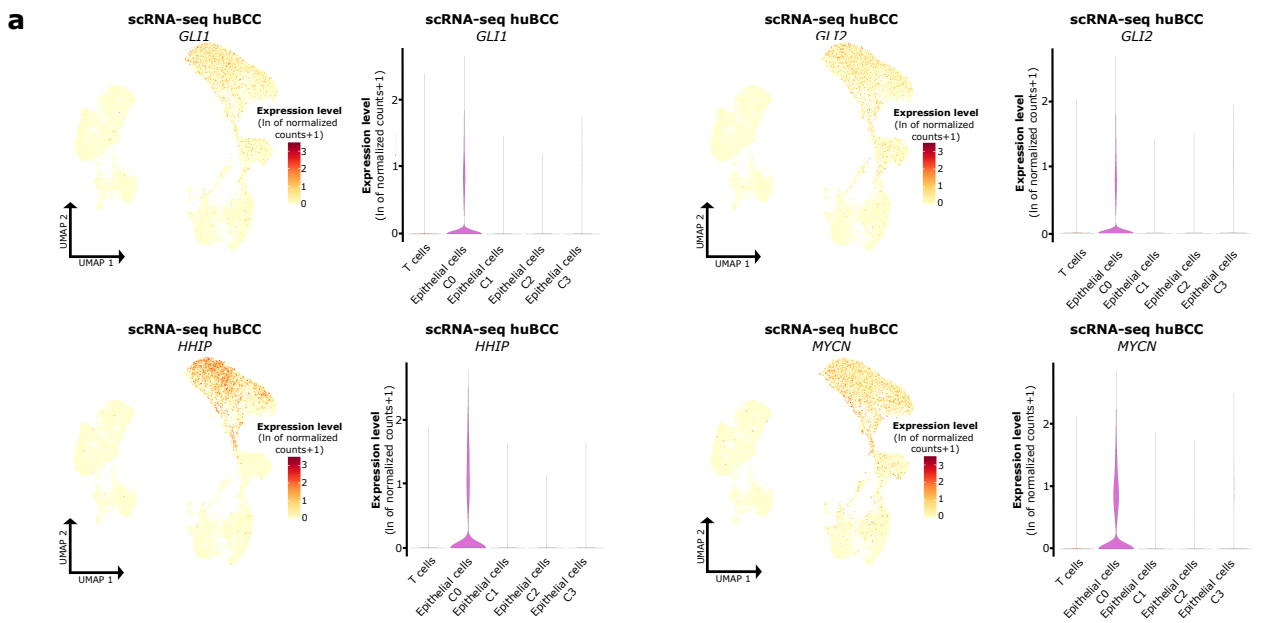
BCC, basal cell carcinoma; DSP, digital spatial profiling; scRNA-seq, single-cell RNA sequencing; DSP-seq, digital spatial profiling sequencing; #, number; %, percent; huBCC, human basal cell carcinoma; UMI, unique molecular identifier; LISI, local inverse Simpson's index.



**Supplementary Fig. 2 Single cell copy-number variation analysis of *KRT14*<sup>pos</sup> epithelial cells.**

Representative CNV heatmaps from inferCNV analysis of *KRT14*<sup>pos</sup> epithelial cell clusters compared to T cells as reference for BCC2 **(a)**, BCC3 **(b)**, BCC4 **(c)**, and BCC5 **(d)**. Arrowheads and rectangles highlight inferred CNVs, after exclusion of gene expression changes shared by the *KRT14*<sup>pos</sup> epithelial cells from the five BCC samples.

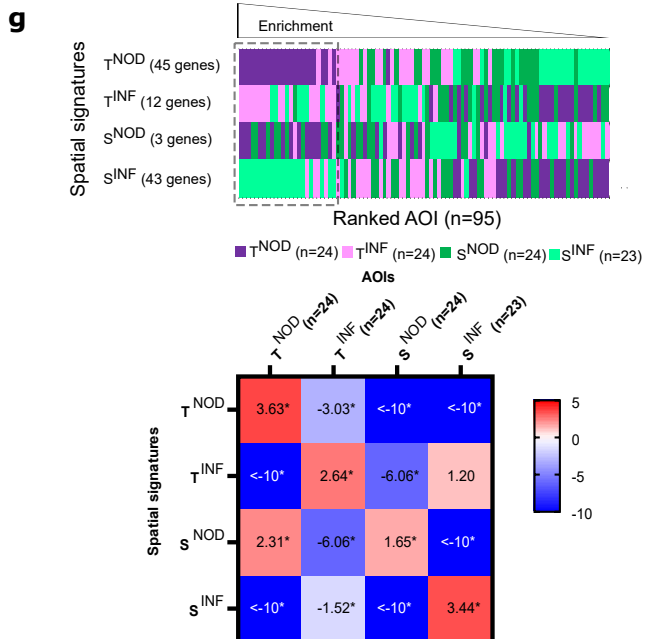
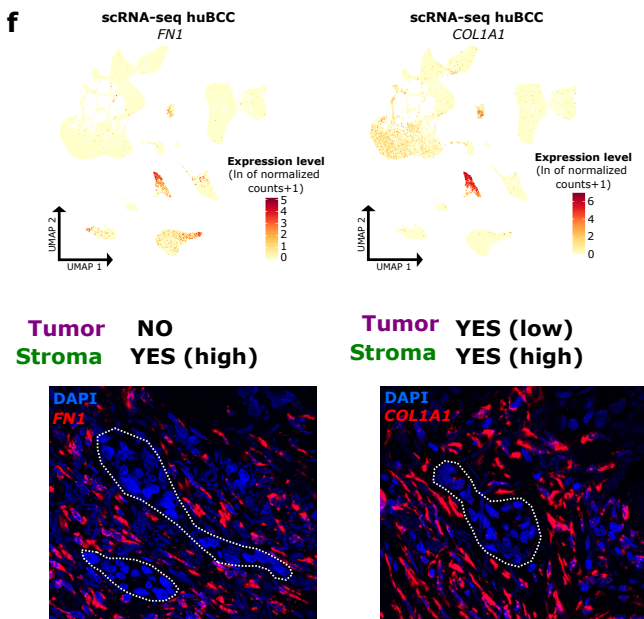
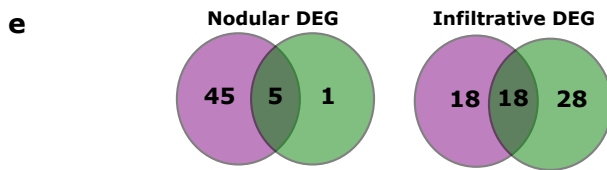
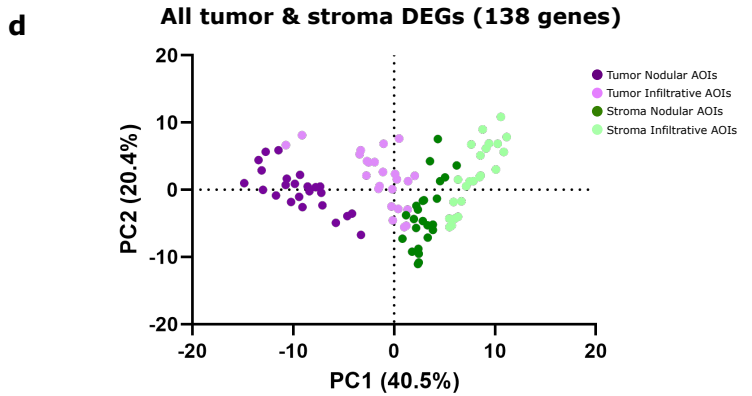
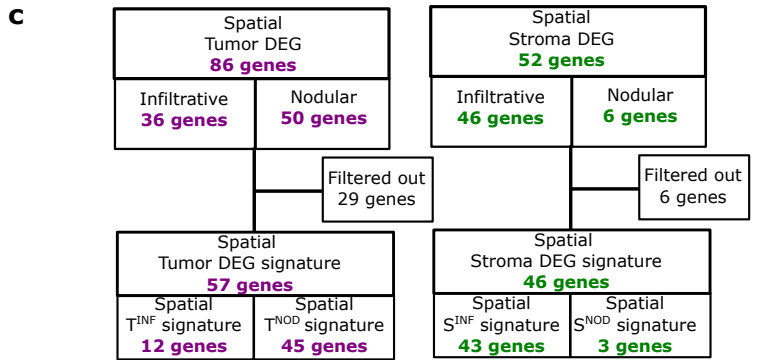
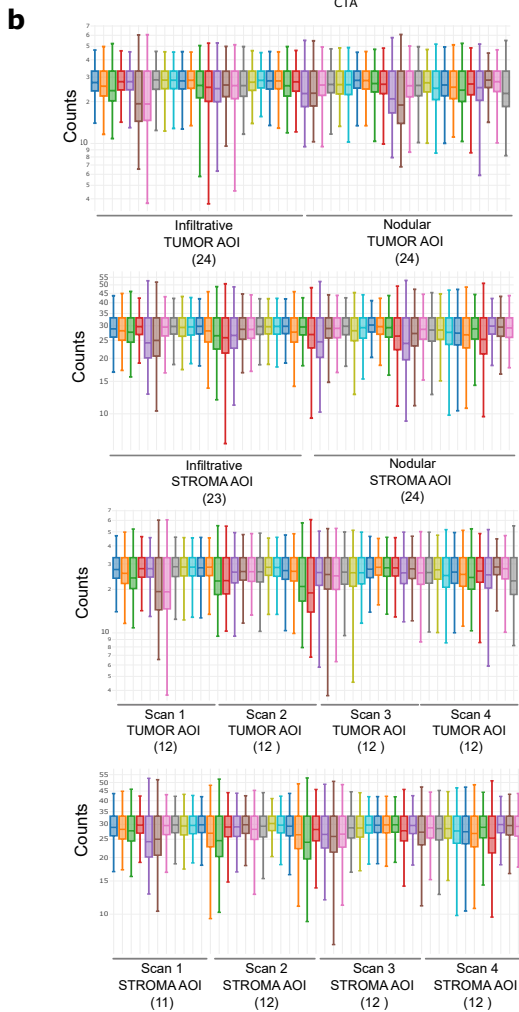
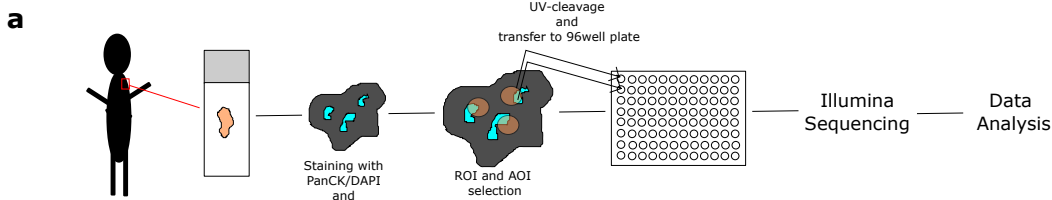
BCC, basal cell carcinoma; CNV, copy number variation.



**Supplementary Fig. 3 Characterization of the non-cycling *KRT14*<sup>pos</sup> epithelial cell subpopulations in scRNA-seq.**

**a)** Expression level of BCC (*GLI1*, *GLI2*, *HHIP*, *MYCN*) marker genes in the epithelial and T cell subpopulations, represented as a color scale overlaid on the UMAP plot (left panels) and as violin plots per cell type (right panels). **b)** Average expression level of the “KEGG Hedgehog signaling pathway” (left panels) and “KEGG basal cell carcinoma” (right panels) signatures in the epithelial and T cell subpopulations, represented as a color scale overlaid on the UMAP plot and as violin plots per cell type. **c)** Average expression level of the “hair follicle” signatures in the epithelial and T cell subpopulations, represented as a color scale overlaid on the UMAP plot (left panels) and as violin plots per cell type (right panels). **d)** Average expression level of the “basal IFE” signatures in the epithelial and T cell subpopulations, represented as a color scale overlaid on the UMAP plot (left panels) and as violin plots per cell type (right panels). **e)** Average expression level of “spinous IFE” and “granular IFE” signatures in the epithelial and T cell subpopulations, represented as a color scale overlaid on the UMAP plot (left panels) and as violin plots per cell type (right panels).

scRNA-seq, single-cell RNA sequencing; huBCC, human basal cell carcinoma; IFE, interfollicular epidermis.



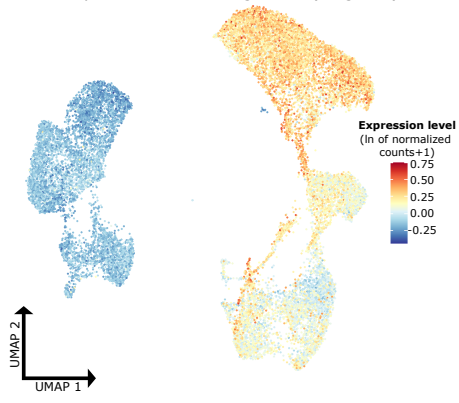


**Supplementary Fig. 4 Establishment of compartment-specific DEG signatures for nodular and infiltrative tumor-stroma interfaces.**

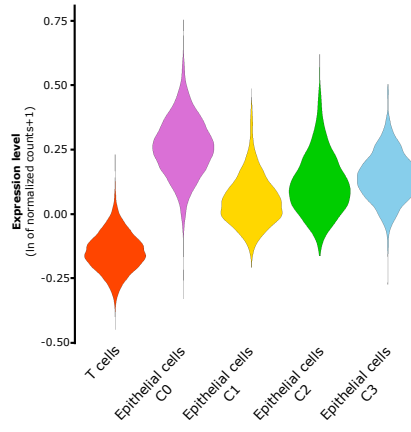
**a)** Schematic of the GeoMx DSP experimental process from tissue collection to data analysis. **b)** Box plots representing the normalized counts per AOI depending on tumor subtype (two upper panels) or scan processing number (two lower panels). **c)** Graphical representation of the establishment of spatial signatures. **d)** PCA plot of the enrichment of all tumor and stroma DEGs in all tumor and stroma AOIs. **e)** Venn diagrams showing the overlap between DEGs in the tumor (purple) and stroma AOIs (green) for each BCC subtype. **f)** Tumor and stromal expression of *FN1* and *COL1A1* determined on scRNA-seq and RNA FISH, illustrating tumor-stroma RNA cross-contamination. Dotted lines highlight the tumor-stroma interface. Scale bars indicate 20  $\mu\text{m}$ . **g)** Ranked individual AOIs according to their enrichment for specific spatial signatures (upper panel). Dotted lines indicate upper quartile (25%) with the highest enrichment. Specificity of individual spatial signatures assessed by the representation of subtype-specific AOI in the 25% most enriched AOIs (lower panel). Positive and negative values indicate over- and under-representation respectively compared to expectations (fold change), based on the cumulative distribution function of the hypergeometric distribution. \* p-value <0.05.

panCK, pan-cytokeratin; CTA, cancer transcriptome atlas; ROI, region of interest; AOI, area of interest; UV-cleavage, ultra-violet cleavage; DEGs, differentially expressed genes; T<sup>NOD</sup>, nodular tumor; T<sup>INF</sup>, infiltrative tumor; S<sup>NOD</sup>, nodular stroma; S<sup>INF</sup>, infiltrative stroma; PC, principal component; PCA, principal component analysis; scRNA-seq, single-cell RNA sequencing; huBCC, human basal cell carcinoma.

**scRNA-seq huBCC**  
Spatial Tumor DEG signature (57 genes)



**scRNA-seq huBCC**  
Spatial Tumor DEG signature (57 genes)

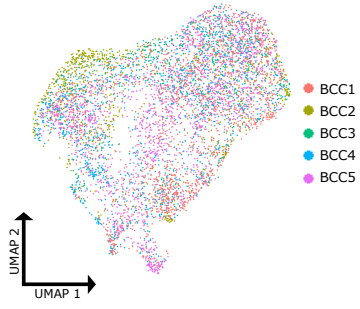


**Supplementary Fig. 5 Spatial signatures map cell subtypes composing tumor-stroma interface in infiltrative BCCs.**

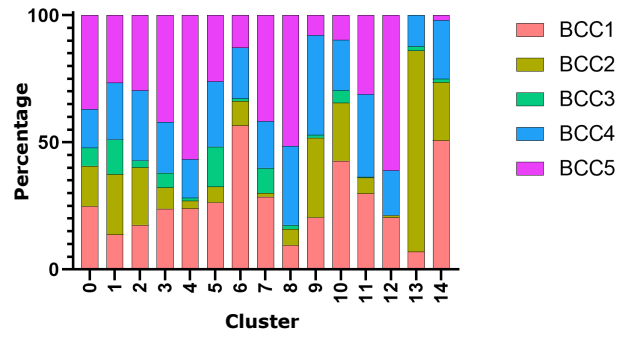
Average expression level of the spatial Tumor DEG signature in epithelial cells (tumor cells and keratinocytes) and T cells of five huBCC samples, represented as a color scale overlaid on the UMAP plot (left panel) and as violin plots per cell type (right panel).

scRNA-seq, single-cell RNA sequencing; huBCC, human basal cell carcinoma; DEG, differentially expressed genes; UMAP, uniform manifold approximation and projection; C, cluster.

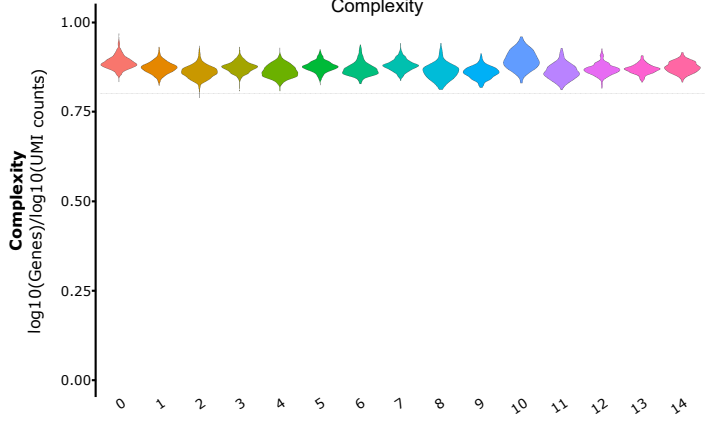
**a** scRNA-seq Tumor Cells huBCC Patient



**Patient representation**



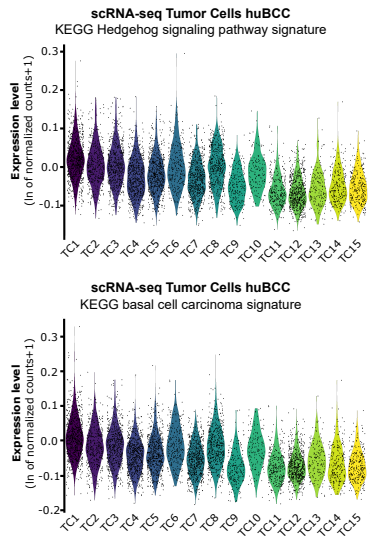
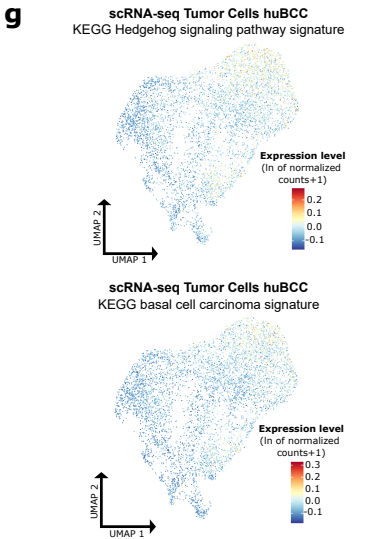
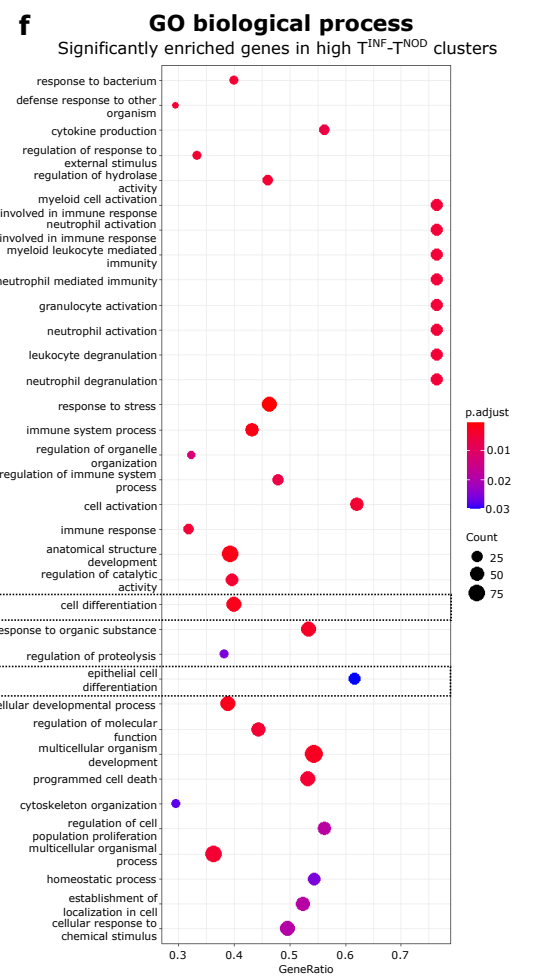
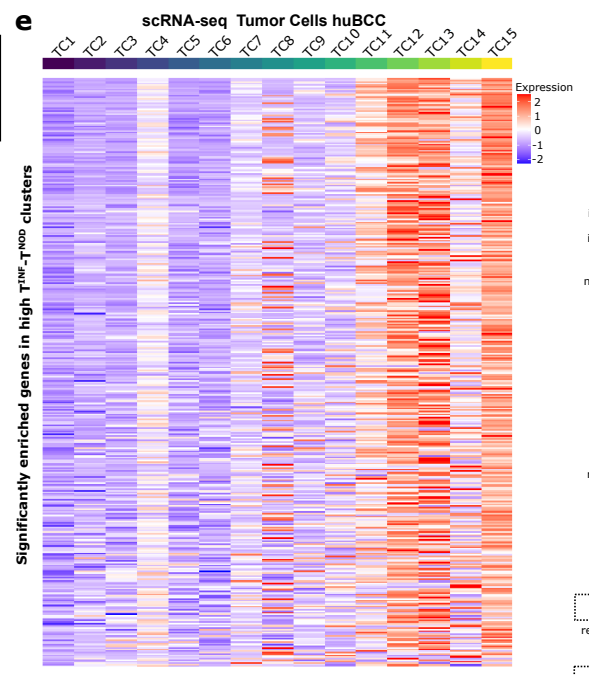
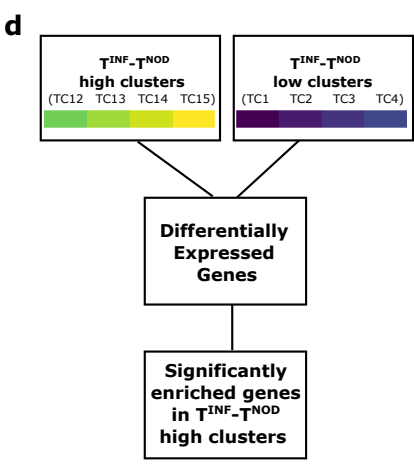
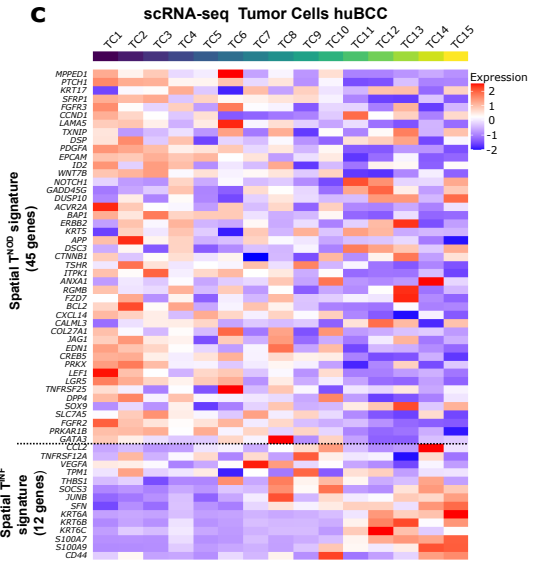
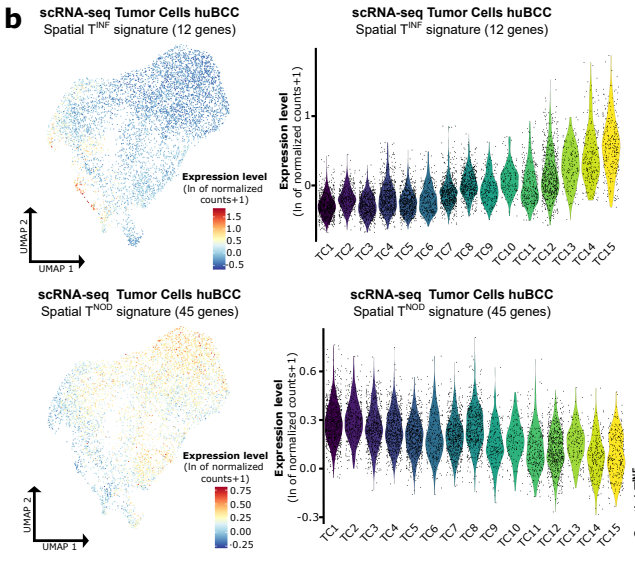
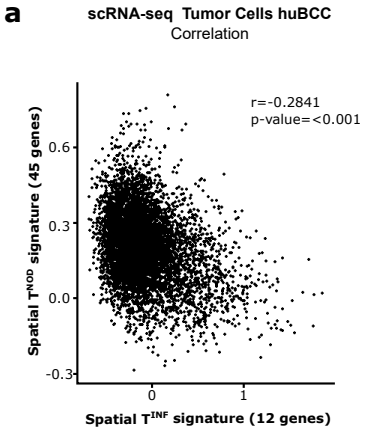
**b** scRNA-seq Tumor Cells huBCC Complexity



**Supplementary Fig. 6 Quality control of the scRNA-seq tumor cell subpopulations.**

**a)** UMAP plot of the tumor cell subpopulations colored according to the huBCC samples (left panel) and bar graph of the scRNA-seq tumor cell subpopulations illustrating the contribution by sample to each cluster (right panel). **b)** Complexity of gene expression in each cluster of the scRNA-seq tumor cell subpopulations, represented as violin plots. Dotted line indicates the expected inferior threshold for satisfactory complexity (0.8).

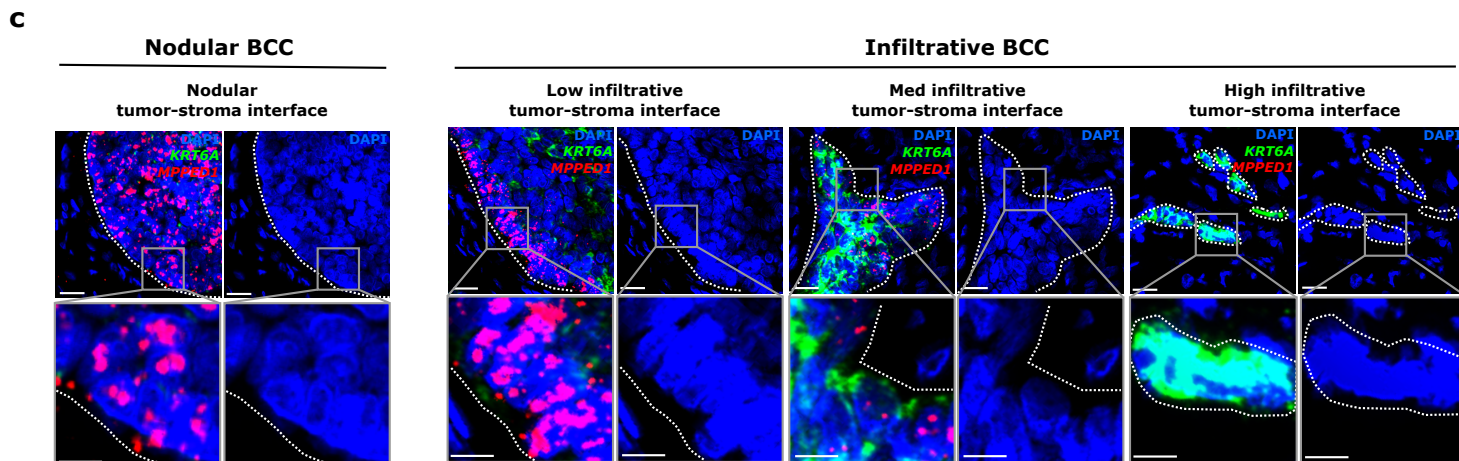
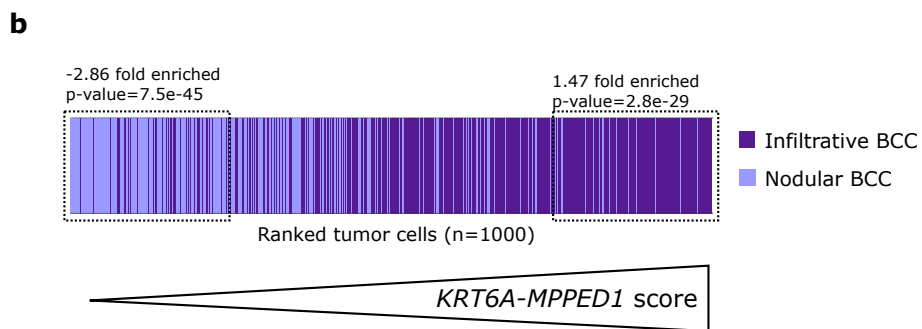
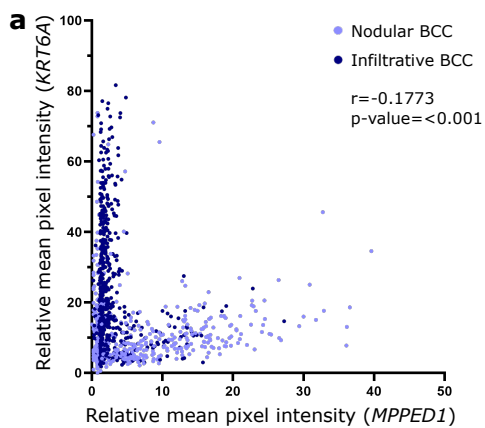
scRNA-seq, single-cell RNA sequencing; huBCC, human basal cell carcinoma; BCC, basal cell carcinoma; UMAP, uniform manifold approximation and projection; UMI, unique molecular identifier.



**Supplementary Fig. 7 Characterization of tumor cell subpopulations within the invasive niche.**

**a)** Correlation analysis between the spatial  $T^{INF}$  and spatial  $T^{NOD}$  signature enrichment scores in individual tumor cells from the scRNA-seq tumor cell subpopulations. R coefficient and p-value were calculated by Spearman correlation test and a two-sided statistical significance test respectively. **b)** Average expression level of the spatial  $T^{INF}$  signature (upper panels) and the spatial  $T^{NOD}$  signature (lower panels) in tumor cell subpopulations of the scRNA-seq dataset, represented as a color scale overlaid on the UMAP plot (left panels) and as violin plots per ranked cluster (right panels). **c)** Heatmap of the average expression level of genes present in the  $T^{NOD}$  and  $T^{INF}$  signatures in tumor cell subpopulations. **d)** Graphical representation of the establishment of the significantly enriched genes in clusters with high  $T^{INF}$ - $T^{NOD}$  enrichment score in the tumor cell subpopulations of the scRNA-seq dataset. **e)** Heatmap of the average expression level of significantly enriched genes in tumor cell subpopulations. **f)** Dot plot showing the GO biological processes enriched in the significantly enriched genes. **g)** Average expression level of the “KEGG Hedgehog signaling pathway” and “KEGG basal cell carcinoma” signatures in tumor cell subpopulations of the scRNA-seq dataset, represented as a color scale overlaid on the UMAP plot and as violin plots per ranked cluster.

scRNA-seq, single-cell RNA sequencing; huBCC, human basal cell carcinoma; BCC, basal cell carcinoma;  $T^{NOD}$ , nodular tumor;  $T^{INF}$ , infiltrative tumor; UMAP, uniform manifold approximation and projection; TC, tumor cluster; GO, gene ontology; p.adjust, adjusted p-value.





**Supplementary Fig. 8 *KRT6A-MPPED1* difference score in tumor cells parallels morphological changes at the tumor-stroma interface.**

**a)** Correlation analysis between *MPPED1* and *KRT6A* relative intensities in individual tumor cells located at the tumor-stroma interface in nodular (N=4) and infiltrative (N=6) BCCs (n=100 cells/sample). R coefficient and p-value were calculated by Spearman correlation test and a two-sided statistical significance test respectively. **b)** Ranked individual cells according to the difference between *KRT6A* and *MPPED1* relative intensities. Dotted lines indicate the lower quartile (25%) (left) with the lowest difference score and the upper quartile (25%) (right) with the highest difference score. Negative and positive values indicate under- and over-representation respectively of infiltrative BCCs compared to expectation (fold change), based on the cumulative distribution function of the hypergeometric distribution. **c)** Representative scan images of Nodular, Low, Med and High infiltrative tumor-stroma interfaces stained with DAPI (blue), *KRT6A* (green), and *MPPED1* (red) probes for RNA FISH. Dotted lines highlight the tumor-stroma interface. Scale bars indicate 20  $\mu\text{m}$  in upper images and 10  $\mu\text{m}$  in zoom areas.

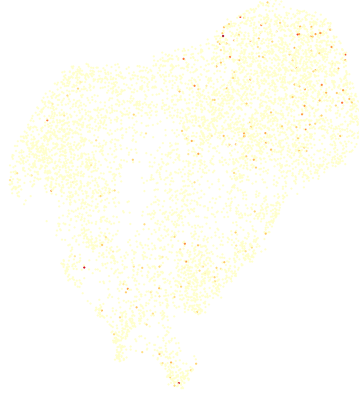
Source data for a) and b) are provided as a Source Data file.

BCC, basal cell carcinoma.

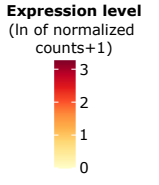
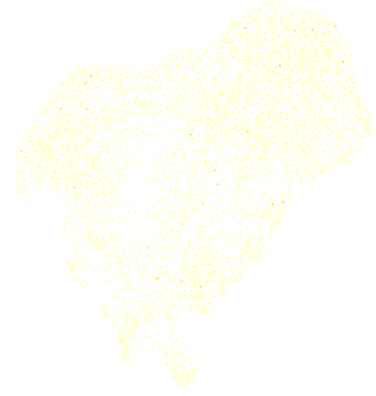
scRNA-seq Tumor Cells huBCC  
*FN1*



scRNA-seq Tumor Cells huBCC  
*POSTN*



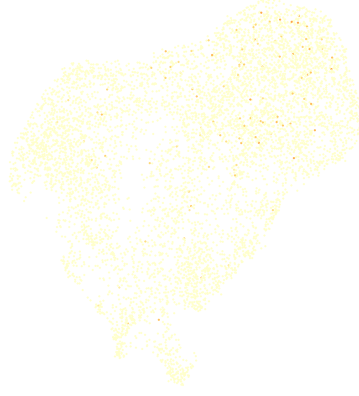
scRNA-seq Tumor Cells huBCC  
*CCN4*



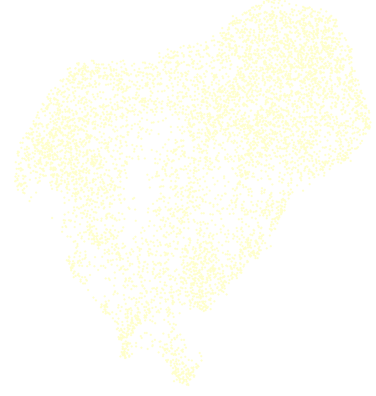
scRNA-seq Tumor Cells huBCC  
*COL3A1*



scRNA-seq Tumor Cells huBCC  
*ADAMTS2*



scRNA-seq Tumor Cells huBCC  
*LRRC15*



UMAP 2  
UMAP 1

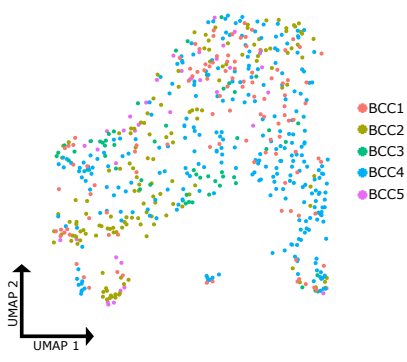
A small coordinate system with two arrows: a vertical arrow pointing up labeled 'UMAP 2' and a horizontal arrow pointing right labeled 'UMAP 1'.

**Supplementary Fig. 9 Tumor cells show little or no expression of known infiltrative BCC-specific marker genes.**

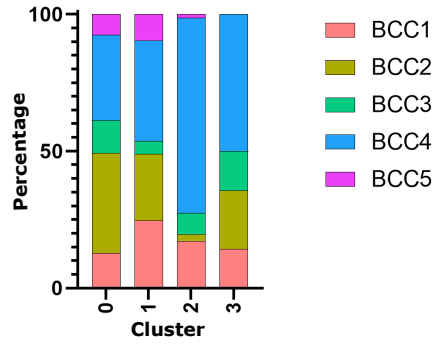
Expression level of known infiltrative BCC-specific marker genes in tumor cell subpopulations of the scRNA-seq dataset, represented as a color scale overlaid on the UMAP plot.

scRNA-seq, single-cell RNA sequencing; huBCC, human basal cell carcinoma; UMAP, uniform manifold approximation and projection.

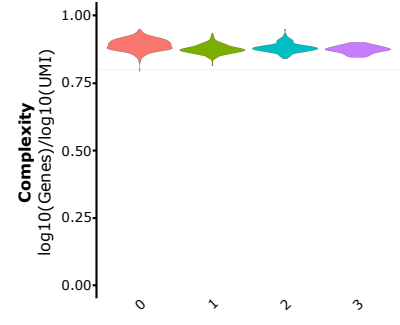
**a** scRNA-seq Fibroblasts huBCC Patient



**Patient representation**



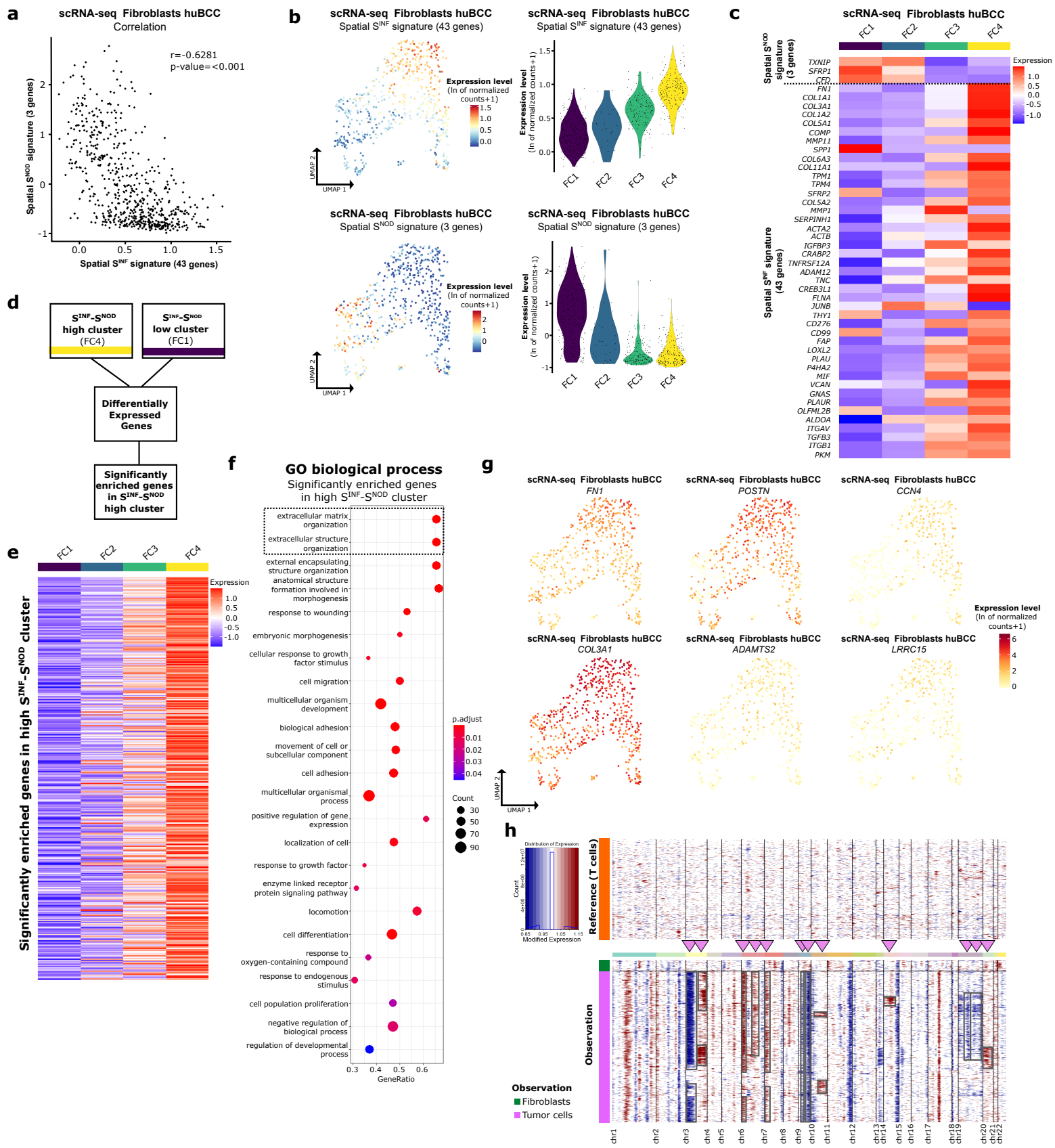
**b** scRNA-seq Fibroblasts huBCC Complexity



**Supplementary Fig. 10 Quality control of the scRNA-seq fibroblast subpopulations.**

**a)** UMAP plot of the fibroblast subpopulations colored according to huBCC samples (left panel) and bar graph of the scRNA-seq fibroblast subpopulations illustrating the contribution by sample to each cluster (right panel). **b)** Complexity of gene expression in each cluster from the scRNA-seq fibroblast subpopulations, represented as violin plots. Dotted line indicates the expected inferior threshold for satisfactory complexity (0.8).

scRNA-seq, single-cell RNA sequencing; huBCC, human basal cell carcinoma; BCC, basal cell carcinoma; UMAP, uniform manifold approximation and projection; UMI, unique molecular identifier.



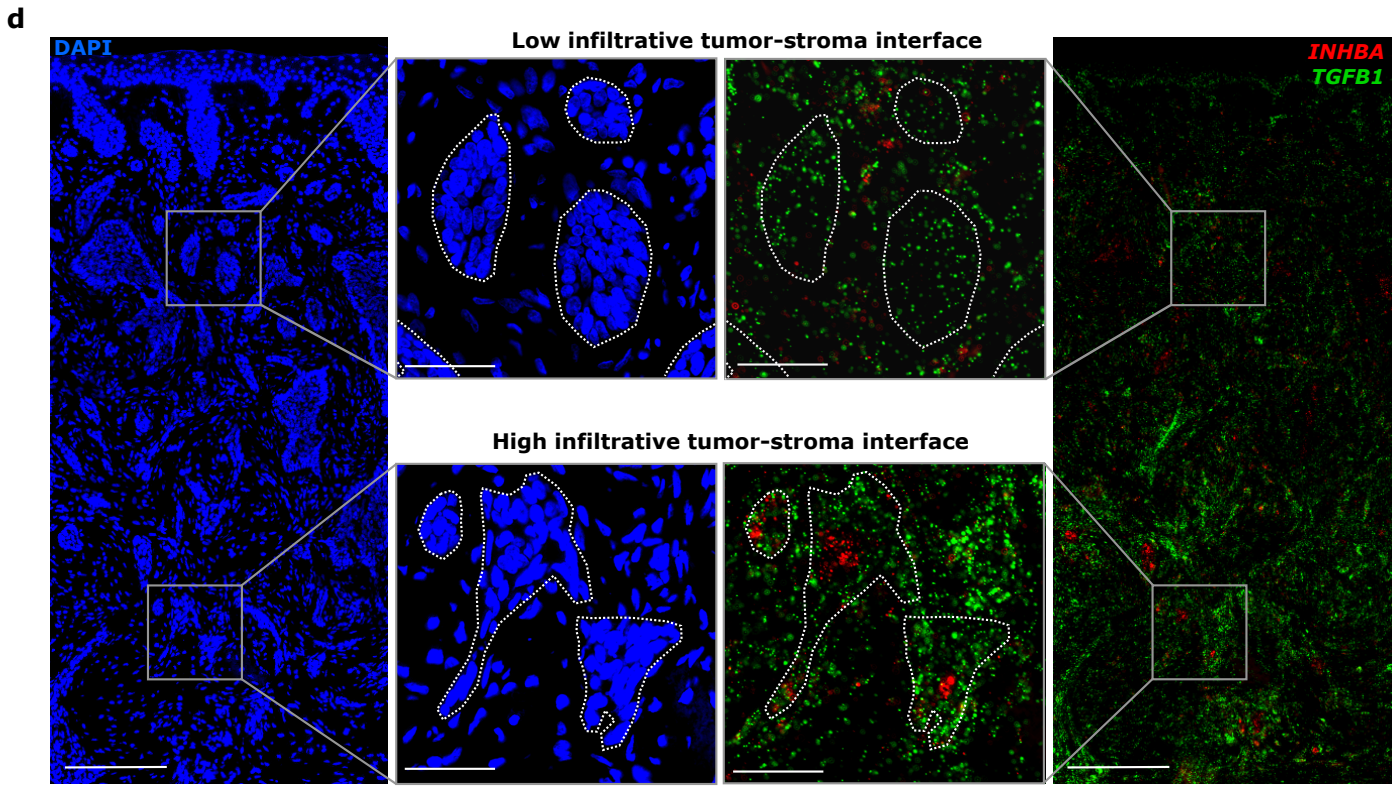
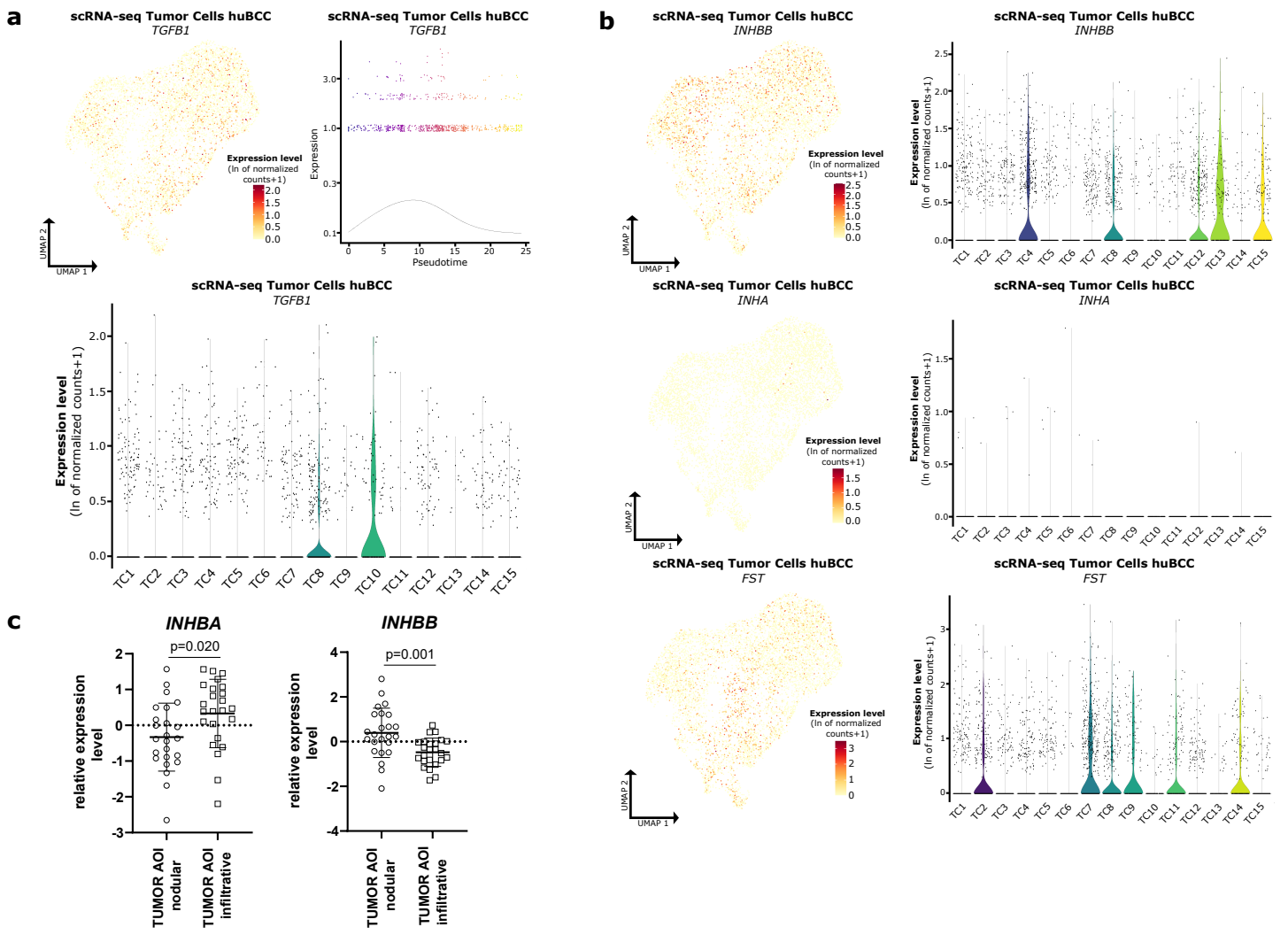
**Supplementary Fig. 11 Characterization of the fibroblast subpopulations within the invasive niche.**

**a)** Correlation analysis between the spatial  $S^{\text{INF}}$  and spatial  $S^{\text{NOD}}$  signature enrichment scores in individual fibroblasts from the scRNA-seq fibroblast subpopulations. R coefficient and p-value were calculated by Spearman correlation test and a two-sided statistical significance test respectively. **b)** Average expression level of the spatial  $S^{\text{INF}}$  signature (upper panels) and spatial  $S^{\text{NOD}}$  signature (lower panels) in fibroblast subpopulations on the scRNA-seq dataset, represented as a color scale overlaid on the UMAP plot (left panels) and as violin plots per ranked cluster (right panels). **c)** Heatmap of the average expression level of genes present in the  $S^{\text{NOD}}$  and  $S^{\text{INF}}$  signatures in fibroblast subpopulations. **d)** Graphical representation of the establishment of the significantly enriched genes in clusters with high  $S^{\text{INF}}-S^{\text{NOD}}$  enrichment score in fibroblast subpopulations of the scRNA-seq dataset. **e)** Heatmap of the average expression level of significantly enriched genes in fibroblast subpopulations. **f)** Dot plot showing the GO biological processes enriched in the significantly enriched genes. **g)** Expression level of known infiltrative BCC-specific marker genes in fibroblast subpopulations of the scRNA-seq dataset, represented as a color scale overlaid on the UMAP plot. **h)** Representative CNV heatmap from inferCNV analysis of tumor cell and fibroblast subpopulations compared to T cells as reference (BCC1). Arrowheads and rectangles highlight gene expression changes that were not shared by the  $KRT14^{\text{pos}}$  epithelial cells from the five BCC samples and thus confidently representing genomic structural changes rather than cell lineage- or cluster-dependent transcriptional programs.

scRNA-seq, single-cell RNA sequencing; huBCC, human basal cell carcinoma;  $S^{\text{NOD}}$ , nodular stroma;  $S^{\text{INF}}$ , infiltrative stroma; UMAP, uniform manifold approximation and

projection; FC, fibroblast cluster; GO, gene ontology; p.adjust, adjusted p-value; chr, chromosome.

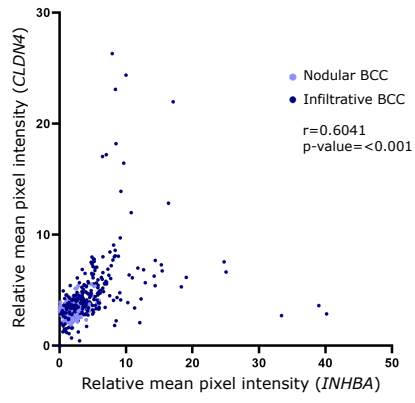
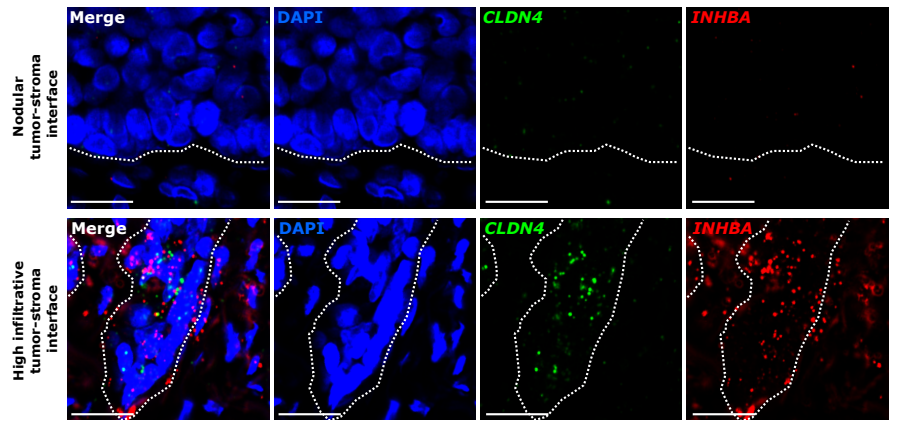
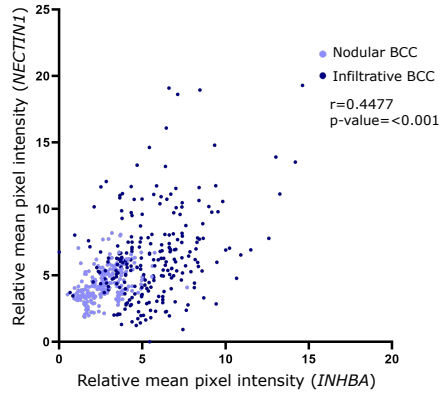
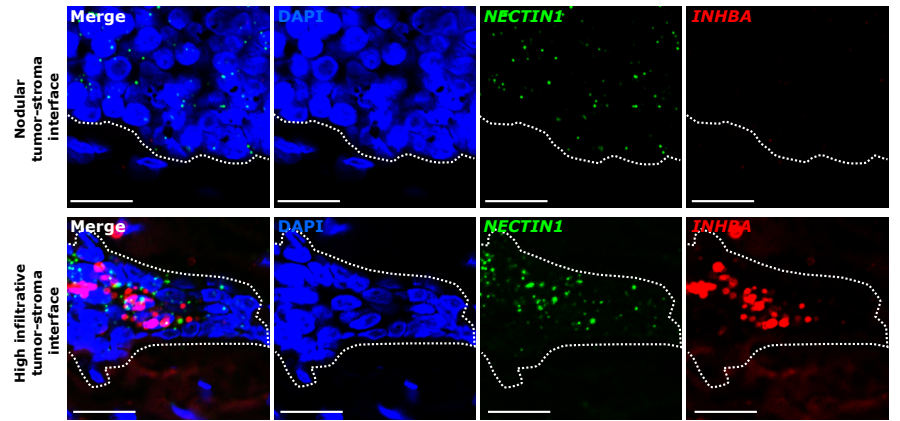
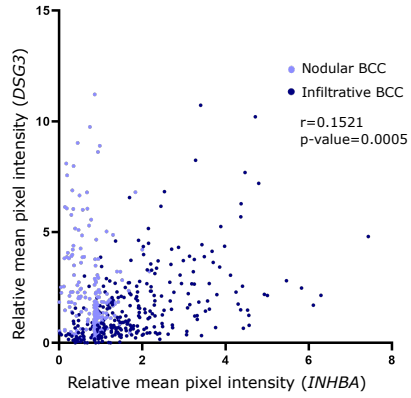
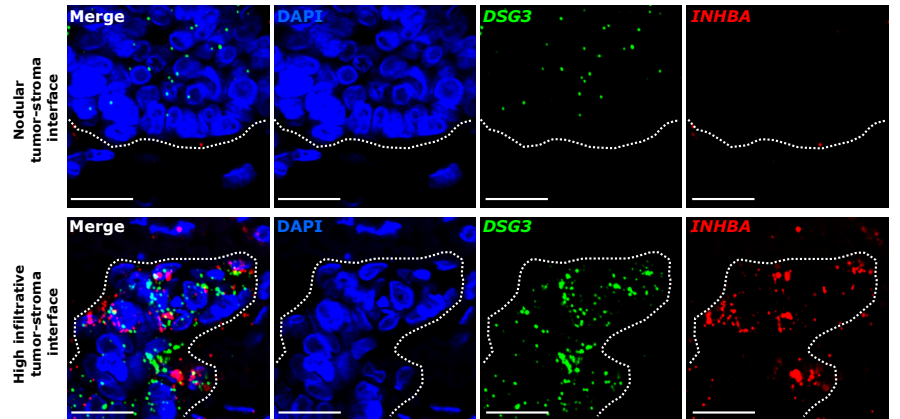




**Supplementary Fig. 12 *INHBA* and *TGFB1* show distinct expression patterns in infiltrative BCCs.**

**a)** Expression level of *TGFB1* in tumor cell subpopulations of the scRNA-seq dataset, represented as a color scale overlaid on the UMAP plot (upper left panel) and as violin plots per ranked cluster (lower panel). Expression level per cell of *TGFB1* along the pseudotemporal trajectory of tumor cell subpopulations (upper right panel). **b)** Expression level of *INHBB*, *INHA* and *FST* in tumor cell subpopulations of the scRNA-seq dataset, represented as a color scale overlaid on the UMAP plot (left panels) and as violin plots per ranked cluster (right panels). **c)** Relative expression levels of *INHBA* and *INHBB* in nodular and infiltrative AOIs obtained from DSP. Horizontal bars represent the mean  $\pm$  SD. P-values calculated using unpaired two-sided Student's t-test. **d)** Representative scan images of an infiltrative BCC section stained with DAPI (blue), *INHBA* (red) and *TGFB1* (green) probes of RNA FISH. Upper and lower zoom areas show tumor-stroma interfaces with distinct Low and High infiltrative morphologies respectively. Dotted lines highlight the tumor-stroma interface. Scale bars indicate 200  $\mu$ m (main panels) and 50  $\mu$ m (zoom panels).

scRNA-seq, single-cell RNA sequencing; huBCC, human basal cell carcinoma; UMAP, uniform manifold approximation and projection; TC, tumor cluster; AOI, area of interest.

**a****b****c****d****e****f**

**Supplementary Fig. 13 *INHBA* expression correlates with marker genes of collective migration in highly infiltrative tumor cells.**

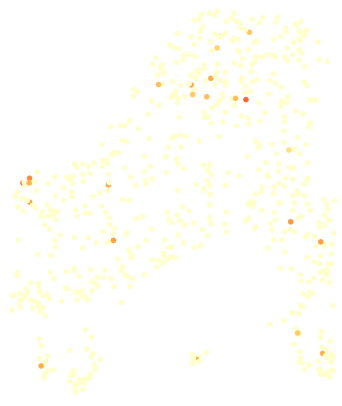
**a)** Correlation analysis between tumor *CLDN4* and *INHBA* relative intensities at the tumor-stroma interface in nodular (N=4) and infiltrative (N=5) BCCs (n≥45 regions/sample). **b)** Representative scan images of Nodular and High infiltrative tumor-stroma interfaces stained with DAPI (blue), *CLDN4* (green) and *INHBA* (red) probes for RNA FISH. **c)** Correlation analysis between tumor *NECTIN1* and *INHBA* relative intensities at the tumor-stroma interface in nodular (N=4) and infiltrative (N=4) BCCs (n≥45 regions/sample). **d)** Representative scan images of Nodular and High infiltrative tumor-stroma interfaces stained with DAPI (blue), *NECTIN1* (green) and *INHBA* (red) probes for RNA FISH. **e)** Correlation analysis between tumor *DSG3* and *INHBA* relative intensities at the tumor-stroma interface in nodular (N=4) and infiltrative (N=5) BCCs (n≥45 regions/sample). **f)** Representative scan images of Nodular and High infiltrative tumor-stroma interfaces stained with DAPI (blue), *DSG3* (green) and *INHBA* (red) probes for RNA FISH.

R coefficients and p-values in a), c) and e) were calculated by Spearman correlation test and a two-sided statistical significance test respectively. In panels b), d) and f), dotted lines highlight the tumor-stroma interface and scale bars indicate 20 μm.

Source data for a), c) and e) are provided as a Source Data file.

BCC, basal cell carcinoma.

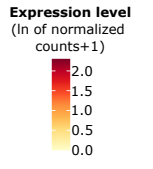
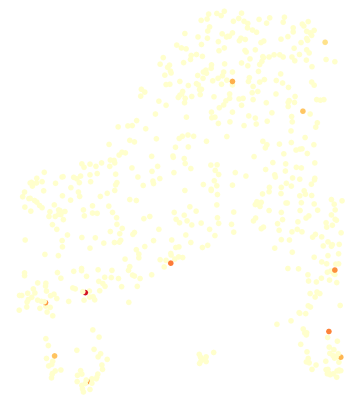
scRNA-seq Fibroblasts huBCC  
*ACVR1B*



scRNA-seq Fibroblasts huBCC  
*ACVR2A*



scRNA-seq Fibroblasts huBCC  
*ACVR2B*

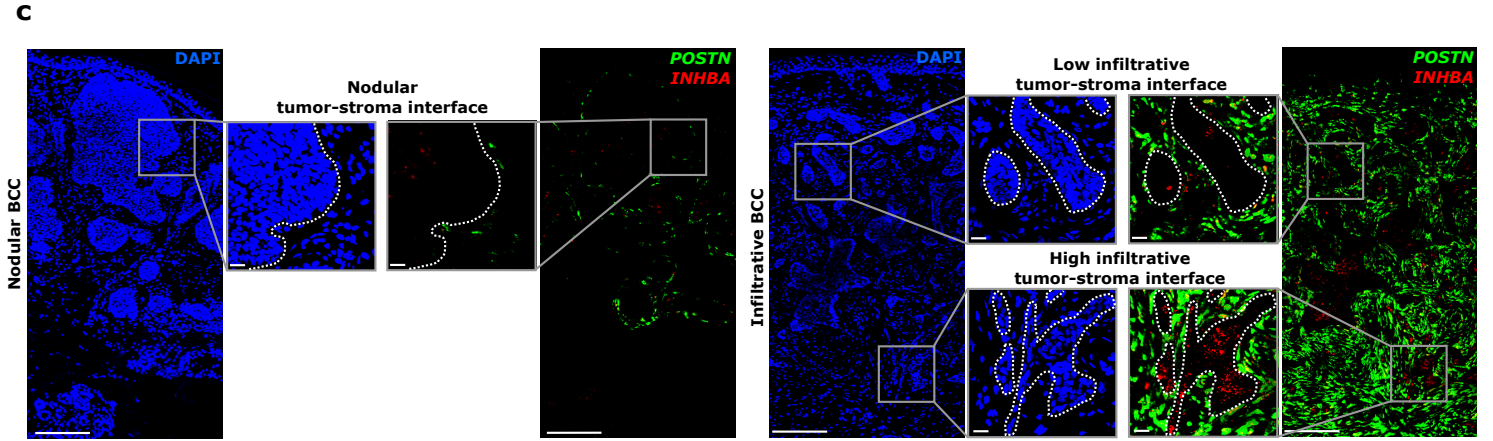
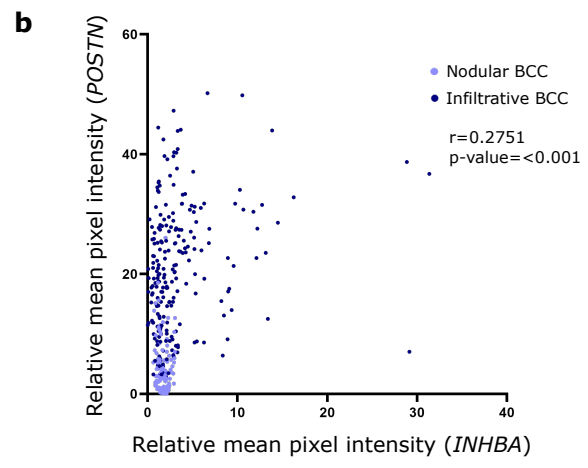
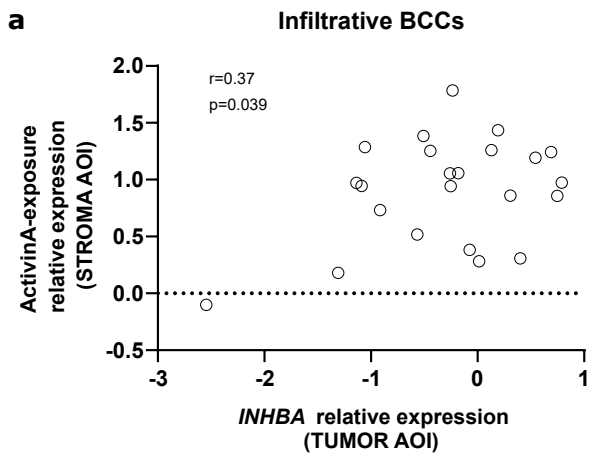


UMAP 2  
↑  
UMAP 1  
→

**Supplementary Fig. 14 Activin A receptors expression in CAFs.**

Expression level of Activin A receptor genes (*ACVR1B*, *ACVR2A* and *ACVR2B*) in fibroblast subpopulations of the scRNA-seq dataset, represented as a color scale overlaid on the UMAP plot.

scRNA-seq, single-cell RNA sequencing; huBCC, human basal cell carcinoma; UMAP, uniform manifold approximation and projection; CAFs, cancer-associated fibroblasts.



**Supplementary Fig. 15 *INHBA* expression in tumor correlates with ECM genes expression in surrounding CAFs.**

**a)** Correlation analysis between the expression of *INHBA* in tumor AOI and Activin A-exposure signature (*FN1*, *COL1A1*, *ACTA2*, *IL6*, *SPP1*) in adjacent stroma AOI of infiltrative BCCs, based on DSP. **b)** Correlation analysis between tumor *INHBA* and adjacent stromal *POSTN* relative intensities in nodular (N=4) and infiltrative (N=8) BCCs (n≥15 regions/sample). **c)** Representative scan images of nodular and infiltrative BCC sections stained with DAPI (blue), *INHBA* (red) and *POSTN* (green) probes of RNA FISH. Upper, intermediate and lower zoom areas show tumor-stroma interfaces with distinct Nodular, Low and High infiltrative morphologies respectively. Dotted lines highlight the tumor-stroma interface. Scale bars indicate 200 μm (main panels) and 20 μm (zoom panels).

R coefficients and p-values in a) and b) were calculated by Spearman correlation test and a two-sided statistical significance test respectively.

Source data for b) are provided as a Source Data file.

AOI, area of interest; BCC, basal cell carcinoma; ECM, extracellular matrix; CAF, cancer-associated fibroblast.